

# On the Breakage of Liquid–Liquid Dispersions in Turbulent Pipe Flow: Spatial Patterns of Breakage Intensity

M. Kostoglou\*

*Division of Chemical Technology, Department of Chemistry, Aristotle University, Univ. Box 116, 541 24 Thessaloniki, Greece*

A. J. Karabelas

*Chemical Process Engineering Research Institute—CERTH, P.O. Box 60361, GR 570 01, Thessaloniki, Greece*

The breakage of droplets in turbulent pipe flow is a subject of great technological interest. The purpose of this work is to take advantage of state-of-the-art theoretical developments and obtain quantitative predictions enhancing our physical understanding of this problem. From this perspective, the subject of the “exact” solutions to an appropriate mathematical model, being recently an issue in the literature, is clarified. Furthermore, the simplest possible mathematical model of the breakage process is derived that retains the complete process parameter dependencies. To implement the model, an appropriate algebraic approach is proposed for the prediction of the radial profiles of key turbulent flow field parameters. This mathematical model adequately relates the breakage pattern in the pipe with the operating process parameters. The results suggest that droplet breakage occurs almost exclusively in an annular region at the periphery of the pipe. Droplets larger than a certain critical size initially have a tendency to break quite rapidly in that region, whereas turbulent diffusion seems to be comparatively slow and cannot spread the fragments into the bulk. This interplay of breakage and diffusion mechanisms seems to lead to initially nonuniform lateral droplet number concentration profiles with rather strong axial (or equivalent time) dependence, over distances of practical significance for process plants. This work clearly suggests that the often-made assumption of uniform conditions in the pipe cross section, regarding size distribution of the droplets that are undergoing breakage, should be reconsidered.

## 1. Introduction

The breakage of droplets in a turbulent flow field is a well-known problem, and it has been addressed extensively in the literature. However, for the case of stirred tanks, it is now well-understood that the nonhomogeneity of the turbulent energy dissipation rate in the flow field is a key feature of the process and must be taken into account in any modeling attempt; the situation is less clear for the turbulent pipe flow, despite the plethora of relevant studies. Traditionally, the pipe flow is considered to offer a much more uniform environment than stirred tanks for the study of breakage phenomena.<sup>1</sup> Of course, for pipe flow, there is the inherent disadvantage of limited fluid residence time (because of the experimental facilities of pipe length, which are limited by necessity), in comparison to the stirred tank geometry. This drawback has not allowed the collection of much-needed droplet evolution data over an adequate pipe length or flow/process time, which would offer valuable information for studies such as this one. Nevertheless, significant studies of liquid dispersions in pipes are still conducted; for instance, turbulent pipe flow recently has been applied to study more-complex droplet phenomena (at rather high concentrations) than just single droplet breakage.<sup>2</sup> In this case, as well as in the somewhat simpler case of dilute dispersions, the spatial pattern of breakage phenomena is certainly a crucial issue in any modeling attempt.

From this brief overview, there is clearly a need to assess the degree of uniformity of the breakage phenomena in turbulent pipe flow. This issue has been already addressed in a series of

two recent papers.<sup>3,4</sup> However, the main focus in these papers is on the derivation of special semianalytical mathematical procedures for the solution of the problem, rather than on examining, in detail, the dependence of the breakage pattern on the physical parameters. To be more specific, in the first paper, results are reported that correspond to strictly localized breakage with no consideration to the influence of turbulent mixing, whereas in the second paper, results are presented for just one set of physical parameters. The similar problem of examining aggregation patterns for the case of aerosols in turbulent pipe flow has also been studied;<sup>5</sup> however, these results cannot be applied to the case of droplet breakage, because there are two major differences between the two problems. First, in the case of aerosol aggregation, the effect of turbulent mixing is insignificant. Second, and most important, the turbulent aggregation rate is only weakly dependent (square root) on the turbulent energy dissipation rate, whereas the corresponding dependence for the breakage rate is very strong. Consequently, this work is motivated by the need to understand the breakage pattern in turbulent pipe flow, which is responsible for the droplet size distribution; the latter, in turn, essentially determines the spatial distribution of the dispersed phase (due to gravity), the practical significance of which is well-known.<sup>6</sup> Note that gravity effects are not considered in this paper, but they will be the subject of future study.

The scope of this work is twofold: (i) to clarify the issue of “exact” solutions to the pipe breakage problem discussed lately, and (most important) (ii) to examine spatial patterns of breakage in the turbulent pipe flow and relate them to the physical conditions, thus setting the stage for more-detailed modeling of the process. The structure of the work is as follows: The

\* To whom correspondence should be addressed. Tel.: +30-2310997767. Fax: +30-2310997759. E-mail: kostoglu@chem.auth.gr.

mathematical problem is outlined first and the issue of “exact” solutions is discussed in some detail. A relatively simple model of the turbulent breakage of droplets in pipe flow then is developed and used (in the results and discussion section) as a tool to improve the understanding of the process.

## 2. Problem Formulation

A quite general form of the equation that describes steady-state convection, diffusion, and fragmentation in the cylindrical geometry is given as follows (here,  $x$ ,  $r$ , and  $z$  are the independent coordinates (i.e., particle volume, radial and axial coordinate, respectively)):

$$u(r) \frac{\partial f(x,r,z)}{\partial z} = \frac{1}{r} \frac{\partial}{\partial r} D(x,r) r \frac{\partial f(x,r,z)}{\partial r} + \int_x^\infty p(x,y;r) b(y,r) f(y,r,z) dy - b(x,r) f(x,r,z) \quad (1)$$

where  $f$  is the particle number density function,  $u$  the velocity,  $D(x,r)$  the diffusion coefficient of the particles of size  $x$ ,  $b(x,r)$  the breakage frequency (rate) of the particle of size  $x$ , and  $p(x,y;r)$  the fragment size distribution resulting from a particle of volume  $y$ . The dependencies of the aforementioned quantities on the spatial coordinate  $r$  are evident in their arguments. The boundary conditions for the aforementioned equation are the symmetry condition at the pipe axis and the no-penetration condition at the wall:

$$\left( \frac{\partial f}{\partial r} \right)_{r=0} = 0 \quad (2a)$$

$$\left( \frac{\partial f}{\partial r} \right)_{r=R} = 0 \quad (2b)$$

where  $R$  is the pipe radius. A quite general initial condition is given as  $f(x,r,0) = f_0(x,r)$ .

## 3. On the Analytical Solution of the Breakage Problem in Turbulent Pipe Flow

The case of constant velocity ( $u(r) = u$ ) with the diffusivity dependent only on particle size ( $D(x,r) = D(x)$ ) and space-independent breakage functions ( $b(x,r) = b(x)$ ,  $p(x,y;r) = p(x,y)$ ) has been examined in detail for the cylindrical geometry (among other geometries), using the separation of variables technique.<sup>7</sup> These authors have argued that the aforementioned form of the problem parameters (velocity, diffusivity, breakage rate, and kernel) is the most general one that allows application of either the separation of variables technique, or eigenfunction expansion, or finite integral transform, or linear operator expansion; in fact, all these procedures should lead to the same result. The final result of that work<sup>7</sup> is a series solution for  $f(x,r,z)$ , where the  $r$  and  $z$  dependencies are expressed in terms of standard functions but the  $x$  dependence is given in terms of functions that must be constructed through recursive integral relations. Formally, this solution can be called “exact”, because the functions can be written in explicit form and no discretization is needed before one attempts to evaluate the integrals. It will be added that, only for some specific cases of  $D(x)$ ,  $b(x)$ , and  $p(x,y)$ , these functions are obtained in closed form.

Nere and Ramkrishna<sup>3</sup> considered a case more general than that of Kostoglou and Karabelas,<sup>7</sup> concerning droplet breakage and diffusion in a turbulent pipe flow. In their approach, the functional dependence of the parameters in eq 1, which is assumed to be representative of turbulent pipe flow, is  $u(r)$ ,  $D(r)$ ,  $p(x,y)$ ,  $b(x,r) = b_1(x)b_2(r)$ . These authors proposed a very

elaborate solution technique of the resulting mathematical problem. The first step of the solution is the discretization in the  $x$ -dimension, using conventional sectional techniques. The rest of the procedure is based (implicitly) on the diagonalization of the system of partial differential equations using linear algebra techniques and the spectral expansion of the resulting self-adjoint operator. The eigenfunctions and eigenvalues of the operator are determined using numerical techniques (i.e., discretization in the  $r$ -dimension). Thus, although the aforementioned authors<sup>3</sup> call their solution “exact”, in contrast to that of Kostoglou and Karabelas<sup>7</sup> (whose solution is at least formally exact), that solution involves discretization in two dimensions and only the third dimension ( $z$ ) is represented by standard functions. In the Appendix, an analytical solution to a simplified formulation of the breakage problem is presented, where spatially uniform velocity, diffusivity, and breakage functions are assumed. This is considered to be the only possible analytical solution for breakage in pipe flow, in the sense that introducing a spatial dependence into at least one of the aforementioned parameters would necessitate the use of numerical techniques.

## 4. A Simple Model for Breakage in Turbulent Flow

It is desirable to develop a simple model that requires limited computational effort, yet is realistic and capable to represent the gross features of the motion and breakage of droplets in turbulent pipe flow, thus permitting an improved understanding of the process. For such a model, the following are required:

(1) The use of a realistic radial distribution (in the pipe cross section) of the velocity, turbulent diffusivity, and turbulent energy dissipation rate.

(2) An expression for the breakage rate and the breakage kernel with functional dependence on the particle size and turbulent energy dissipation rate.

(3) A mathematical procedure to solve the resulting system of partial integral-differential equations at the required level of detail.

These issues will be examined one by one in the following subsections.

**4.1. Radial Profiles of Turbulent Quantities.** Although, in principle, direct numerical simulation of the turbulent flow in a pipe is possible, it presents serious difficulties, for practical problems, using present-day computational resources.<sup>8</sup> Furthermore, this type of modeling is not compatible with the scope of the present work. Thus, the radial profiles can be obtained based on the well-known Reynolds Average Navier Stokes (RANS) approach. The turbulent RANS models are briefly assessed, starting from the simplest one. The zero-equation models are capable of providing the velocity and turbulent diffusivity radial distributions but no information for the distribution of turbulent energy dissipation rate ( $\epsilon$ ), which is the most important parameter for the problem at hand. The one-equation models (equation for the kinetic energy) can provide the radial distribution of  $\epsilon$ , but their use in the literature is very limited and they are often criticized for not leading to results better than the zero-equation models.<sup>8</sup> Thus, the simplest model for the present purpose is the well-known two-equation  $k-\epsilon$  model.

A convenient way to compute the radial distributions of the turbulent quantities based on the  $k-\epsilon$  model is the use of a commercial computational fluid dynamics (CFD) code. The conservation equation for the droplets can be included in the CFD code, leading to a model that involves a heavy computational load; alternatively, the radial distribution functions obtained from the CFD code can be used in eq 1. However, in

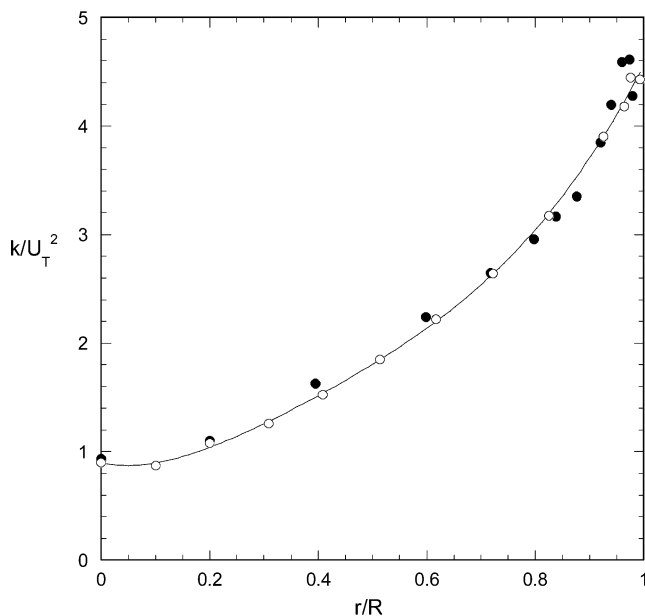


**Figure 1.** Radial profiles of the dimensionless quantity  $k/U_T^2$ : (○) experimental data<sup>12,13</sup> for  $Re = 21\,800$  and (●) experimental data<sup>12,13</sup> for  $Re = 500\,000$ . Solid curve represents the fit to the data.

both cases, the procedure is considered unacceptable, because a computationally demanding two-dimensional problem must be solved to determine one-dimensional profiles that correspond to fully developed flow. The problem is that the CFD codes cannot be solved directly for the one-dimensional problem (radial profiles) of fully developed flow. Thus, a one-dimensional boundary value problem must be solved to obtain the radial distribution of velocity  $u(r)$  and of turbulent quantities  $\epsilon(r)$  (turbulent energy dissipation rate),  $k(r)$  (turbulent kinetic energy), and  $\nu_T(r)$  (turbulent kinematic viscosity). A comprehensive review of versions of the aforementioned general model and a rather extensive assessment based on comparison with results from the experiments (for  $u$ ,  $k$ ,  $\nu_T$ ) and direct numerical simulation (DNS) (for  $\epsilon$ ) can be found in the literature.<sup>9</sup> Although a particular version of the model<sup>10</sup> was finally proposed, which seemed to show better performance than the more widely used model<sup>11</sup> (e.g., for a breakage application<sup>3</sup>), the results reveal large discrepancies among the models. In addition, although the velocity predictions are very good, the comparison of predictions with experimental and DNS data for the other variables is unsatisfactory. However, even the zero-equation mixing length model can give good results for the velocity. The key question raised here is whether this type of elaborate model is really necessary for the relatively simple pipe flow case that is under consideration. Inspired by the limited success of the theoretical models and the relatively small variation that certain dimensionless quantities exhibit, with respect to Reynolds number  $Re$ , the following procedure is followed to determine the  $\nu_T$  and  $\epsilon$  profiles (at a level appropriate for the scope of the present work). Experimental data<sup>12,13</sup> for the dimensionless quantity  $k/U_T^2$  for  $Re = 21\,800$  and  $500\,000$  are shown in Figure 1.  $U_T$  is the friction velocity, which is defined as

$$U_T = \sqrt{-\frac{R}{2\rho} \frac{dp}{dz}} \quad (3)$$

where  $\rho$  is the density of the continuous phase and  $dp/dz$  is the pressure drop along the pipe. It is obvious that the difference between the two sets of data is smaller than the scatter of the

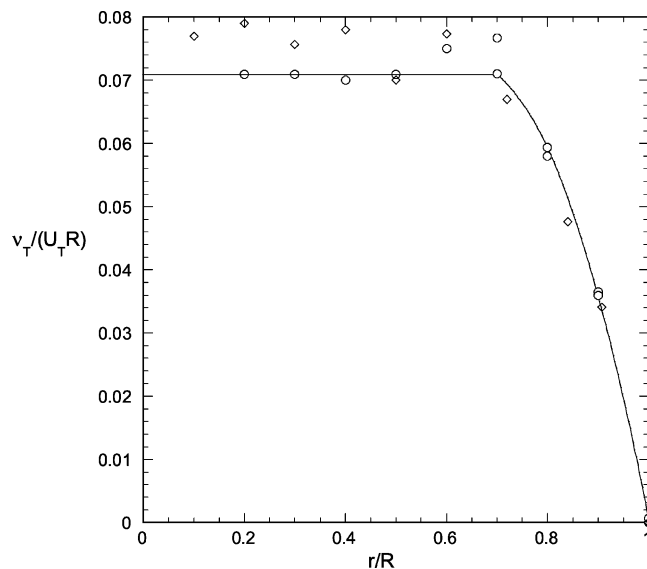


**Figure 2.** Radial profiles of the dimensionless quantity  $\nu_T/(U_T R)$ : (○) experimental data<sup>12</sup> for  $Re = 50\,000$  and (◇) experimental data<sup>12</sup> for  $Re = 500\,000$ . Solid curve represents the fit to the data.

data. Thus, a fifth-order curve (shown in Figure 1) may be fitted to represent all the data (assuming independence of Reynolds number). In this way, all the information of the  $k$ -behavior close to the wall (which is the most important region for the  $\epsilon$ -distribution) is lost and cannot be recovered using the experimental data; indeed, not only is the data resolution poor, but their consistency close to the wall also is subject to criticism. Thus, a theoretical model seems to be needed to reconstruct the near-wall behavior of the kinetic energy distribution. For this purpose, the most successful<sup>9</sup> version of the  $k$ - $\epsilon$  model<sup>10</sup> is used. The final equation for  $k$  is

$$\frac{k}{U_T^2} = \left[ 0.894 - 0.9996\left(\frac{r}{R}\right) + 11.976\left(\frac{r}{R}\right)^2 - 20.148\left(\frac{r}{R}\right)^3 + 17.033\left(\frac{r}{R}\right)^4 - 4.2\left(\frac{r}{R}\right)^5 \right] \left[ 1 - \exp\left(-\frac{y^+}{70}\right) \right] \quad (4)$$

where  $y^+$  is the dimensionless distance from the wall ( $y^+ = (R - r)U_T/\nu$ , where  $\nu$  is the molecular kinematic viscosity). A similar procedure is followed for the eddy viscosity data. The measurements of Laufer<sup>12</sup> for  $Re = 50\,000$  and  $500\,000$  are shown in Figure 2. A relatively insignificant effect of  $Re$  on the radial profile of the quantity  $\nu_T/(U_T R)$  is observed. Thus, this profile is also assumed to be independent of  $Re$ . Although this assumption may not be so good in this case, it is nevertheless interesting that the fitting curve in Figure 2 seems to be closer to the experimental data than any of the elaborate ( $Re$ -dependent) theoretical models.

The fitted expressions for  $\nu_T$  are

$$\frac{\nu_T}{U_T R} = 0.71 \quad \left( \text{for } \frac{r}{R} \leq 0.7 \right) \quad (5a)$$

$$\frac{\nu_T}{U_T R} = -0.1761 + 0.7642\left(\frac{r}{R}\right) - 0.5875\left(\frac{r}{R}\right)^2 \quad \left( \text{for } \frac{r}{R} > 0.7 \right) \quad (5b)$$

The radial distribution of turbulent diffusivity can be obtained directly from the eddy viscosity radial distribution using the simple rule<sup>3</sup>

$$D = \nu_T + \nu$$

The second term of the right-hand side (molecular viscosity  $\nu$ ) is added to avoid the zero diffusivity at the wall, but its contribution is practically negligible. The turbulent energy dissipation ( $\epsilon$ ) radial profile can be determined by substituting eqs 4 and 5 for  $k$  and  $\nu_T$ , respectively, into the following equation and solving for  $\epsilon$ :

$$\nu_T = 0.09 \left[ 1 - \exp\left(-\frac{y^+}{70}\right) \right] \frac{k^2}{\epsilon} \quad (6)$$

The resulting expression for  $\epsilon$  gives the qualitatively expected radial profile of  $\epsilon$  in all cases. In addition, the  $\epsilon$  profile determined by the aforementioned procedure, compared with one given elsewhere<sup>5</sup> (obtained using a CFD code for a particular case of turbulent air pipe flow), is observed to be quite similar.

The radial velocity profile is not computed based on the fitted eddy viscosity profile, but rather from a zero-equation model, using the combined eddy diffusivities of Reinhard and Van-Driest.<sup>14</sup> This approach was shown to predict the experimental data of Laufer accurately.<sup>12</sup> Thus, for given values of pipe radius and average velocity, the friction coefficient is obtained from the Colebrook equation. The latter is used to compute the pressure drop, friction velocity (using eq 3), and the radial profiles, as described previously.

**4.2. Breakage Functions.** Having a model available for the turbulent quantities, the next step is to choose a realistic set of breakage rate and kernel functions. There is a great variety of proposed forms for these functions in the literature. More specifically, the breakage rate is generally accepted to be an increasing function of droplet size, but the proposed kernels exhibit remarkable variation, even in their gross features. Regarding the breakage kernel, it was considered in early modeling efforts that there is a rather sharp cutoff to the breakage rate, corresponding to the so-called “maximum stable size”. In the past 10–15 years, there has been significant experimental evidence, supported by theoretical arguments, that a maximum stable size may not really exist (at least with the meaning initially attached to it). Instead, the evidence suggested that a continuous slow decrease of the droplet size occurred. Alternatively, one may assume that the “maximum stable size” exists but it has a tendency to decrease slowly with breakage time. From the theoretical point of view, several expressions have been developed over the years for the breakage rate. For the case of droplets with viscosity comparable to that of the continuum phase, the method introduced by Luo and Svendsen,<sup>15</sup> which is based on the statistical approach to homogeneous turbulence, has been used quite extensively in the literature. Nevertheless, several drawbacks of this approach have been noted and corrected,<sup>16,17</sup> and a further improvement and generalization has been reported.<sup>18</sup> The breakage rates resulting from this theory are in agreement with the experimental data behavior previously described. Indeed, the breakage process seems to proceed in two stages; i.e. at first, the initial large droplet breaks very fast to a size (reminiscent of the “maximum” stable size) that is almost independent of the initial droplet size, followed by a very slow size reduction with time. The expressions for the breakage rate are rather complicated, but it has been shown<sup>18</sup> that there is a much simpler expression<sup>19</sup> leading to the same qualitative behavior. This expression can be used for the purposes of the present work:

$$b(x) = \frac{1}{c_1} \left( \frac{d}{c_2} \right)^{5/3} \exp \left[ -\frac{\sqrt{2}}{(d/c_2)^3} \right] \quad (7)$$

where  $c_1 = \sigma^{0.4} \rho^{-0.4} \epsilon^{-0.6}$ ,  $c_2 = \sigma^{0.6} \rho^{-0.6} \epsilon^{-0.4}$ ,  $d$  is the particle diameter ( $d = (6x/\pi)^{1/3}$ ), and  $\sigma$  is the dispersed continuous-phase interfacial tension.

Regarding the breakage kernels, the situation is still not clear. Almost every possible type of kernel has been proposed in the literature. A trend in the past was to use a type of algorithmic kernel that was not related directly to physicochemical parameters of the system; multiple breakage kernels and binary kernels with preference for equal or for unequal sizes are some of the choices that can be found in the literature. In the approaches based on the statistical theory of turbulence, binary breakage is considered, with the kernel changing from one of unequal size fragments to another of equal size as the droplet diameter decreases. For consistency with the breakage rate described in eq 7, kernels based on statistical theories will also be used in this work and binary breakage will be assumed. The exact shape of the breakage kernel is not relevant at this point (only the fragment number per breakage event is of interest), because of the level of approximation of the particle size distribution that will be applied.

It is important to notice that, recently, a very extensive set of experimentally obtained particle size distributions of emulsion droplets undergoing breakage in an emulsifier was presented and analyzed in a series of papers.<sup>20–22</sup> This work involves levels of  $\epsilon$  much larger than those typical for stirred tanks (and, of course, for pipe flow) and with low values of surface tension and, correspondingly, with much smaller droplet sizes than those encountered in the present application (1–50  $\mu\text{m}$ , versus sizes on the order of millimeters). Despite these differences, the aforementioned results are considered useful for understanding the basic breakage mechanism. With regard to the maximum stable droplet size and the breakage rate function, the findings<sup>21</sup> are absolutely compatible with the results of the breakage theories, based on the statistical theory of turbulence previously outlined. The situation is quite different for the breakage kernel. The experimental results<sup>22</sup> indicate breakage to many droplets (from 10 for low-viscosity droplets to 300 for high-viscosity droplets). Most of these droplets are satellite drops that result from the instability of the neck connecting the two main daughter droplets. Breakage kernels representing this particular breakage pattern have been used in the past.<sup>23</sup> The size of the satellite drops seems to be dependent only on the hydrodynamic conditions and not on the parent droplet size; thus, their existence may not be important for the droplet size range considered in the present work or for the case of a stirred tank. In any case, although it seems that the breakage rate given by the existing theories is reliable, much work still remains to be done regarding the breakage kernel.

A basic mathematical feature of eq 7 (and of the corresponding equations from the other models, based on the statistical theory of turbulence) is that it is not separable in the sense of  $b(x, \epsilon) = b_1(x)b_2(\epsilon)$ . In contrast, the relation used by Nere and Ramkrishna,<sup>3</sup> is separable; it was derived<sup>24</sup> directly from experimental data, using an inverse problem approach, which is a technique for which there has been recently renewed interest.<sup>25</sup> Equation 7 is a sharply changing function of  $\epsilon$ . For example, a 1-order-of-magnitude decrease of  $\epsilon$  leads to a drastic reduction (up to 8 orders of magnitude) in the breakage rate, and, in addition, the breakage rate practically exhibits a type of low- $\epsilon$  cutoff point. On the other hand, the exponent of  $\epsilon$  in the breakage rate used by Nere and Ramkrishna<sup>3</sup> is just 2.11, which



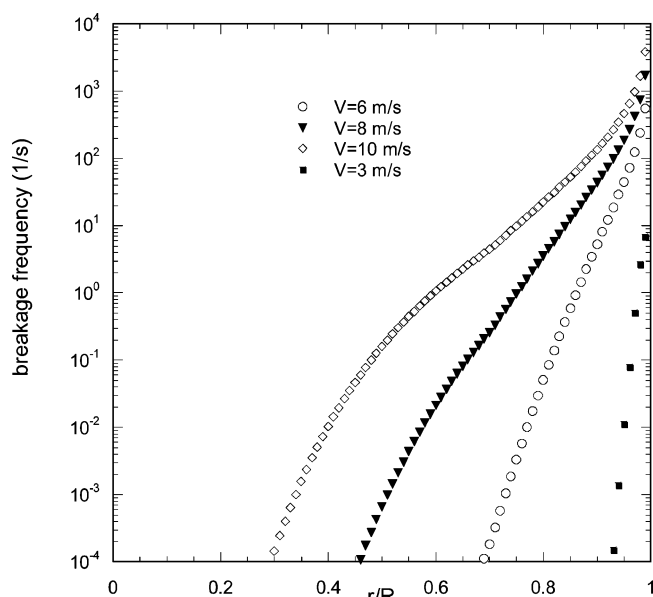


**Figure 3.** Radial profile of the breakage frequency for droplets with a diameter of 2 mm and a surface tension of 0.05 N/m in a pipe with a radius of 0.13 m.

renders the  $\epsilon$ -distribution of lesser significance, in comparison to the present work. Note that the breakage rate function effectively acts as an extremely nonlinear filter to the radial  $\epsilon$  profile, further increasing the radial nonuniformity of the breakage phenomenon. To demonstrate this fact, the radial profiles of the breakage rate for droplets with  $d = 2$  mm and  $\sigma = 0.06$  N/m are shown in Figure 3 for water flow in a pipe of radius  $R = 0.13$  m and for several fluid velocities. It is evident that considerable breakage occurs only in the region close to the wall, whereas in the core of the pipe, there is practically no breakage. This trend is, of course, inconsistent with the general belief that pipe flow is appropriate for studying breakage under fairly uniform cross-sectional conditions. It is further noted that the extreme nonlinearity of eq 7 renders the accuracy of the  $\epsilon$  profile of rather limited importance, providing further justification for the simplified approach used in this work.

**4.3. Solution of Breakage Equation.** To complete the simplified tool, for understanding the spatial breakage distribution in turbulent pipe flow, the population balance (eq 1) must be solved. However, because of the fact that the scope here is to understand the gross features of the process, while keeping the model as simple as possible, the so-called “monodisperse” approximation will be used. The essence of this approximation is the assumption that all the droplets in each point and at each moment of time have the same size. Note that, although this is an inexact assumption, it is expected that the results from the locally monodisperse distribution will be very similar to the real average size of the complete distribution. In any case, this level of approximation can lead to a reliable estimation of the local breakage extent and of the spatial pattern of breakage in turbulent pipe flow. The resulting set of equations that must be solved (obtained by multiplying eq 1 by  $x^i$  ( $i = 0, 1$ ) and integrating both sides from 0 to  $\infty$ ) is as follows:

$$u(r) \frac{\partial N}{\partial z} = \frac{1}{r} \frac{\partial}{\partial r} D(r) r \frac{\partial N}{\partial r} + b\left(\frac{M}{N}\right) N \quad (8)$$

$$u(r) \frac{\partial M}{\partial z} = \frac{1}{r} \frac{\partial}{\partial r} D(r) r \frac{\partial M}{\partial r} \quad (9)$$

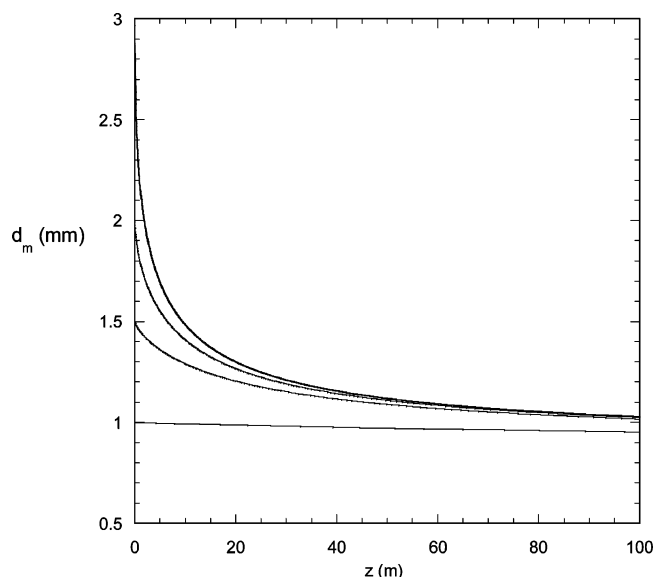


**Figure 4.** Evolution of the cross-sectional average droplet diameter ( $d_m$ ) along the pipe for several values of initial size:  $d_0 = 1.0, 1.5, 2.0$ , and  $3.0$  mm. (Other parameters:  $R = 0.13$  m,  $\sigma = 0.05$  N/m,  $V = 4$  m/s.)

The monodisperse particle size is computed as  $x = M/N$ , and the second term of the right-hand side of eq 8 must be neglected for  $N = 0$ . In the case of a cross-sectionally uniform inlet distribution of particles ( $M = M_0$ ), the second of the aforementioned equations has the solution  $M = M_0$  everywhere, so that only the first equation must be solved. In any case, the second equation is not dependent on the first one and can be solved using a separation-of-variables technique. However, from the computational point of view, the simultaneous numerical solution of both equations is preferable. These equations are discretized in the radial direction, using second-order finite differences. A stiff semi-implicit integrator (explicit integrators are not appropriate, because of the velocity profile) with self-adjustable step and specified accuracy (set to  $10^{-5}$ ) is used for integration in the  $z$ -direction of the resulting system of ordinary differential equations.

## 5. Results and Discussion

As a base case for the present results, one may consider water flow in a pipe of radius  $R = 13$  cm, and dispersed low-viscosity oil with a surface tension of  $\sigma = 0.05$  N/m. The evolution along the pipe of the cross-sectional average of the “monodisperse” droplet diameter  $d_m$  for several values of the initial droplet diameter  $d_0$  is shown in Figure 4 (the average water velocity,  $V$ , is 4 m/s). This scenario is similar to that for batch breakage. Furthermore, it seems that there is an “attractor” droplet size; indeed,  $d_m$  initially has a tendency to be reduced very fast to a value relatively similar to the “attractor” size and then a slow size reduction phase follows. Note that droplets initially larger than the attractor size soon “forget” their initial diameter as they approach the attractor size. In addition, those droplets smaller than the “attractor” droplets do not break at all. The evolution of the average diameter  $d_m$  for the base case for several values of the average water velocity and an initial droplet diameter of  $d_0 = 2$  mm is shown in Figure 5. For small liquid velocities, there is no breakage at all; breakage has a tendency to increase with increasing velocity. It is evident that the basic feature of the velocity effect (related to the  $\epsilon$  increase in the pipe) is the reduction of the attractor droplet size. It is interesting how fast the breakage of the entering droplets has a tendency to be (almost instantaneous at the scale of the figure), leading from

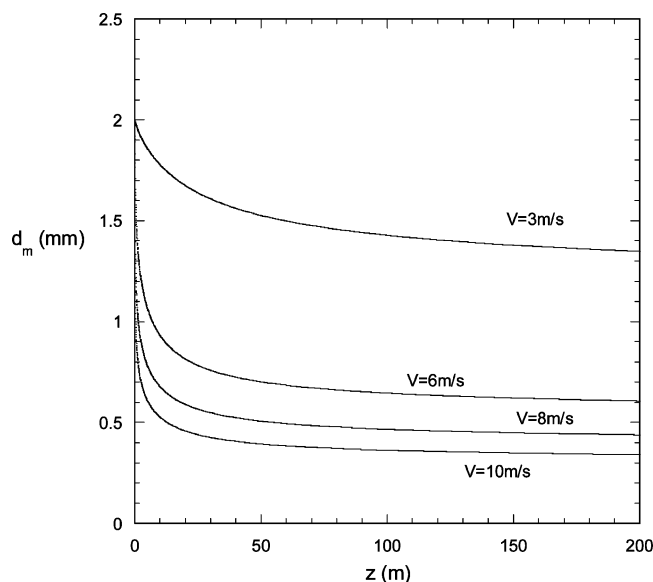


**Figure 5.** Evolution of the cross-sectional average droplet diameter ( $d_m$ ) along the pipe for several values of the average water velocity ( $V = 3\text{ m/s}$ ). Cross-sectionally uniform droplet source. (Other parameters:  $R = 0.13\text{ m}$ ,  $\sigma = 0.05\text{ N/m}$ ,  $d_o = 2\text{ mm}$ .)

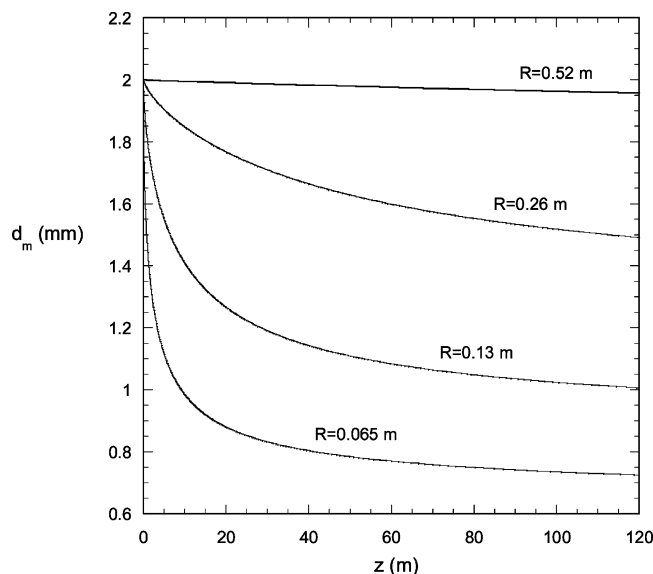


**Figure 6.** Evolution of the cross-sectional average droplet diameter ( $d_m$ ) along the pipe for several values of the pipe radius  $R$ . Cross-sectionally uniform droplet source. (Other parameters:  $V = 4\text{ m/s}$ ,  $\sigma = 0.05\text{ N/m}$ ,  $d_o = 2\text{ mm}$ .)

a droplet diameter  $d_o$  to droplet sizes similar to the “attractor” size. Thus, the water velocity greatly affects the extent of breakage for a given pipe length. This is not a trivial result, because the residence time in the pipe (breakage time) is inversely proportional to velocity  $V$  but the dependence of the breakage rate on  $V$  is so strong that dominates the process. The influence of the radius of the pipe on the evolution of  $d_m$  for a given water velocity ( $V = 4\text{ m/s}$ ) is shown in Figure 6. As expected, as the radius of the pipe increases, the extent of breakage (the “attractor” droplet size) decreases, and, actually, for the largest pipe in Figure 6, the rate of breakage is insignificant.

The preceding discussion has involved the effect of key process parameters on the evolution of the cross-sectionally averaged droplet diameter. However, it is of particular interest to examine the spatial breakage patterns that lead to a particular droplet evolution. To understand the origin of  $d_m$  evolution,

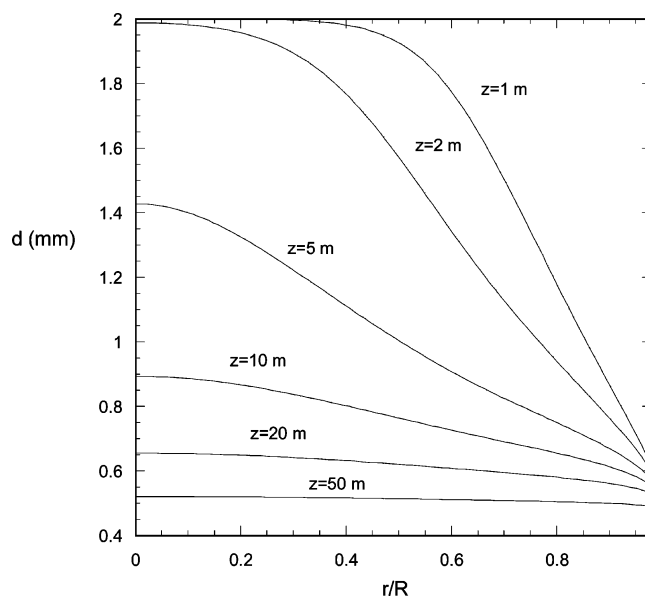


**Figure 7.** Radial profiles of the monodisperse droplet diameter ( $d$ ) at several positions  $z$  along the pipe. Cross-sectionally uniform droplet source. Other parameters:  $R = 0.13\text{ m}$ ,  $\sigma = 0.05\text{ N/m}$ ,  $d_o = 2\text{ mm}$ ,  $V = 8\text{ m/s}$ .)

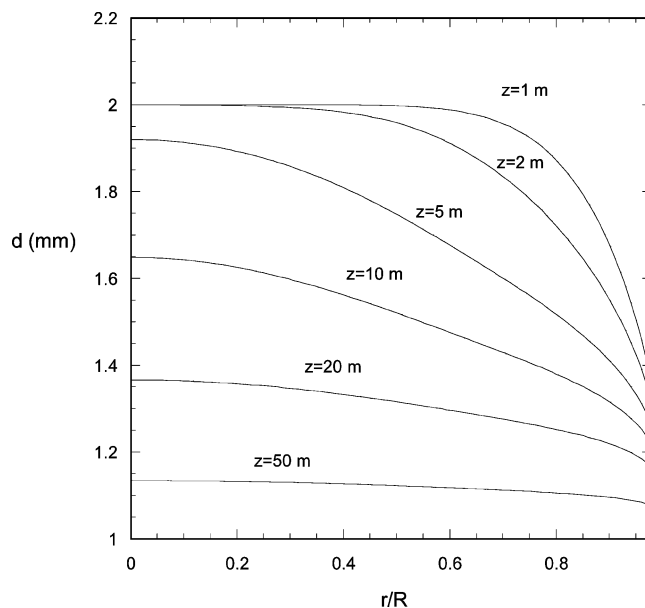


**Figure 8.** Radial profiles of monodisperse droplet diameter ( $d$ ) at several positions  $z$  along the pipe. Cross-sectionally uniform droplet source. (Other parameters:  $R = 0.13\text{ m}$ ,  $\sigma = 0.05\text{ N/m}$ ,  $d_o = 2\text{ mm}$ ,  $V = 4\text{ m/s}$ .)

some spatial profiles of the droplet diameter are presented. Such profiles for the base case with an inlet droplet size of  $d_o = 2\text{ mm}$  and a velocity of  $V = 8\text{ m/s}$  are shown in Figure 7 at several positions  $z$  along the pipe. By examining the first position ( $z = 1\text{ m}$ ), it is evident that the droplets at the periphery of the pipe have undergone extensive breakage, and, in particular, close to the wall, they have already approached the “attractor” size, whereas the droplets in the core retain their initial size. At  $z = 1\text{ m}$ , the droplets are essentially located at their initial  $r$ -position (at the inlet), because there is not enough time for the diffusion to act. Farther downstream (for larger values of  $z$ ), the observed reduction of droplet size in the core of pipe is not due to local breakage but rather to the transfer of small droplets from the periphery due to turbulent diffusion. As the residence time increases ( $z$  increases), the breakage decreases, because of the smaller size of the remaining droplets; therefore, the diffusion prevails, leading to uniform radial droplet

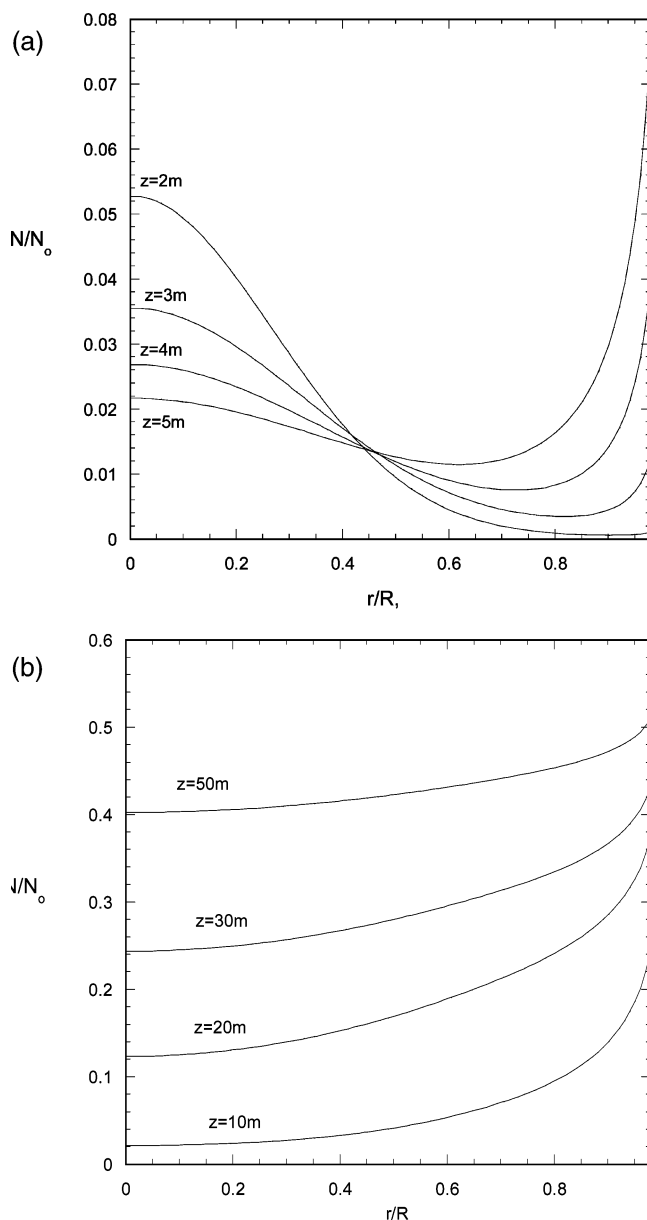


**Figure 9.** (a),(b). Radial profiles of monodisperse droplet diameter ( $d$ ) at several positions  $z$  along the pipe for localized droplet source: (a)  $z = 2, 3, 4$ , and  $5$  m; (b)  $z = 10, 20, 30$ , and  $50$  m. (Other parameters:  $R = 0.13$  m,  $\sigma = 0.05$  N/m,  $d_o = 2$  mm,  $V = 8$  m/s.)

size profiles. The results in Figure 8 are quite similar to those in Figure 7, although they correspond to a slower water velocity ( $V = 4$  m/s). The only difference is that breakage is restricted to a smaller peripheral region (see the  $z = 1$  m curve) and the approach to the “attractor” size close to the wall is more gradual.

A better understanding of the interplay between breakage and diffusion can be obtained by studying the case of a nonuniform inlet profile. In this case, droplet size profiles are not appropriate to provide information on the process, and it is better to present the evolution of dimensionless number concentration profiles. Figures 9a and 9b correspond to exactly the same conditions as those in Figure 8; however, the droplets enter the pipe not from the entire cross section, but rather from a disk at the center with a radius that is 10% of the pipe radius. Initially, the diffusion “spreads” the steep concentration profile at the entrance (e.g.,  $z = 2$ ). In this case, diffusion is much more efficient in the bulk than that in spreading the peripheral small droplets to the pipe core, because of the shape of the turbulent diffusivity

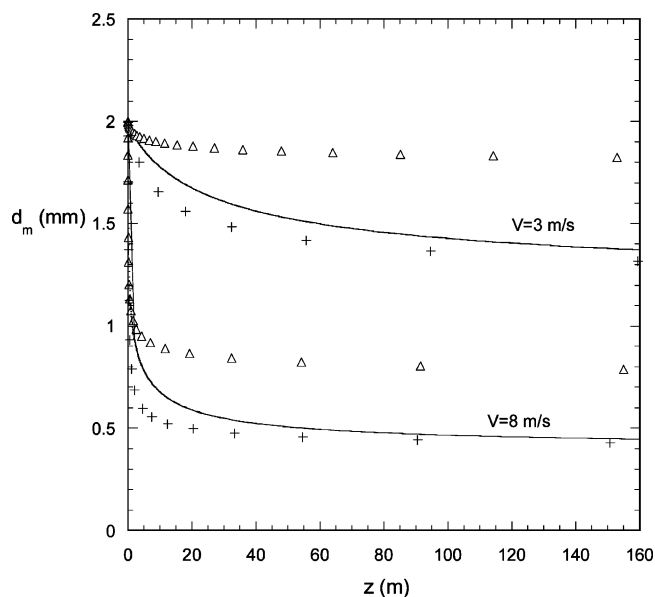


**Figure 10.** Comparison of the actual evolution of  $d_m$  (solid line) with the two asymptotes corresponding to ( $\Delta$ ) no mixing and (+) perfect mixing for two values of water velocity. (Other parameters:  $R = 0.13$  m,  $\sigma = 0.05$  N/m,  $d_o = 2$  mm.)

profile. As  $z$  increases, spreading continues; however, at the wall region, a rather sharp increase in the number concentration appears, because droplets generated there have insufficient time to diffuse back to the core, due to the small local values of diffusivity. With increasing distance  $z$ , the core initial nonuniformity has a tendency to disappear but the wall nonuniformity has a tendency to increase. For distances farther downstream (Figure 9b), the small droplets close to the wall diffuse back toward the core of the pipe, which, as already explained, leads progressively to a uniform radial distribution of droplet number concentration.

According to Kostoglou,<sup>26</sup> the ratio of the diffusion to breakage rate has a tendency to determine the degree of lateral mixing of the droplets in turbulent pipe flow. In the limiting case of a small value of this ratio (no mixing at all), the process can be considered to be a series of non-interacting batch processes. In the other limiting case (a large value of the ratio—perfect mixing), the process can be approximated by a batch breakage process, using the average value of  $\epsilon$ . It is of interest to examine here the particle size evolution for practical situations, where the ratio of the two rates does not remain constant. The simulated evolution of the cross-sectional average diameter is shown in Figure 10, together with the two limiting cases of no mixing and perfect mixing, for the base case and two values of the velocity  $V$ . Initially, the realistic evolution is very similar to the no-mixing case, but it has a gradual tendency to approach the perfect-mixing asymptote. This is considered a very important result; it suggests that, for intensive breakage regions (i.e., close to the injection point of large droplets), the uniform  $\epsilon$ -approximation is definitely wrong, whereas it is a fairly good approximation for large breakage times and/or pipe lengths. It is further suggested that experimental studies that are aimed at determining the “maximum stable droplet diameter” or the equivalent “attractor” size should take into account these trends in designing the experimental setup and selecting appropriate experimental conditions.

According to the present work, the breakage of droplets mainly occurs in a region at the solid walls. This implies that the breakage efficiency increases as the ratio of surface to volume of the flow equipment increases, which explains the

capability of the static mixers to produce fine dispersions, even for a very small pipe length.

## 6. Conclusions

The scope of the present work is the clarification of the droplet breakage pattern in turbulent pipe flow. This is pursued by developing and examining, in detail, the simplest possible model that is capable of representing the salient features of the breakage process; the latter is a combination of some extremely nonlinear mechanisms or sub-processes induced by the radial distribution of the turbulent energy dissipation rate and of the breakage frequency function. The present analysis suggests that breakage occurs almost exclusively at the periphery of the pipe. In addition, in accordance with the latest breakage theories, two periods of breakage are identified; i.e. the first is very fast and reduces the initial droplet size to a size more or less independent of the initial one, whereas in the second period, the particles (having completely “forgotten” their initial state) very slowly approach smaller sizes.

Furthermore, initially, during the period of “intense” breakage, there seems to be insufficient time for turbulent diffusion to act and the phenomena are quite localized (different particle sizes at each radial location). However, during the “slow” size reduction period, the turbulent diffusion rate is greater than the breakage rate, which leads to the development of uniform particle size and lateral concentration profile in the pipe. Consequently, the often-made assumption of fairly uniform conditions in the turbulent pipe flow seems to be valid only “far” from the droplet injection point (i.e., at a distance where the intense breakage has essentially finished). It may be added that exploiting the pattern of turbulent breakage in pipes, which is revealed in the present work, facilitates the development of computationally efficient detailed models of the process.

## Appendix. The Only Possible Analytical Solution for Breakage in Turbulent Pipe Flow

The zeroth-order approximation to the problem assumes a uniform velocity profile (standard plug-flow approximation), a uniform diffusivity (also a usual approximation), and spatially uniform breakage functions  $b(x)$  and  $p(x,y)$  (which is a very poor approximation). Under these conditions, the spatial non-uniformity of the breakage problem is dependent only on the nonuniformity of the inlet conditions. For radially uniform inlet condition ( $f_0(x,r) = f_0(x)$ ), the problem degenerates to the well-known zero-dimension (batch) breakage equation. The spatial dependency is strictly due to the inlet spatial distribution. The simplified problem can be solved using the techniques described elsewhere<sup>7</sup> (applying Neumann instead of Dirichlet conditions) to obtain

$$f(x,r,z) = \sum_{i=1}^{\infty} T_i(x,z) \frac{2J_0(\lambda_i r)}{R^2 J_0^2(\lambda_i R)} \exp\left[-\lambda_i^2 \left(\frac{D}{u}\right) z\right] \quad (\text{A1})$$

where  $J_0$  and  $J_1$  are the Bessel functions of first type (zero and first order, respectively). The notation  $\lambda_i$  is used for the  $i$ th root of the equation  $J_1(\lambda_i R) = 0$  (starting from  $\lambda_1 = 0$ ). Here,  $T_i(x,t)$  is the solution of the batch breakage equation:

$$\frac{\partial T_i(x,z)}{\partial z} = \int_x^{\infty} b(y)p(x,y)T_i(y,z) dy - b(x)T_i(x,z) \quad (\text{A2})$$

with the initial condition

$$T_i(x,0) = \int_0^R f_0(x,r) r J_0(\lambda_i r) dr \quad (\text{A3})$$

In the particular case of a separable inlet condition  $f_0(x,r) = f_0(x)A(r)$ , the aforementioned solution can be simplified considerably and can also be written in separable form:

$$f(x,r,z) = T(x,z) \sum_{i=1}^{\infty} a_i \left[ \frac{2J_0(\lambda_i r)}{R^2 J_0^2(\lambda_i R)} \right] \exp\left[-\lambda_i^2 \left(\frac{D}{u}\right) z\right] \quad (\text{A4})$$

where

$$a_i = \int_0^R A(r) r J_0(\lambda_i r) dr \quad (\text{A5})$$

where  $T(x,z)$  is the solution of the batch breakage equation for  $T(x,0) = f_0(x)$ . Equation A4 is simply the product of the solutions of the batch breakage equation and the diffusion-convection equation. The same result was erroneously proposed<sup>3</sup> for the general case of the spatially variable-dependent breakage rate, but it is actually valid only for the case considered here. For several combinations of breakage functions and  $f_0(x)$ , an analytical solution for  $T(x,z)$ —and, correspondingly, for  $f(x,r,z)$ —can be obtained.

Another analytical solution, but only for the total number concentration, can be determined for the case of breakage rate of the form  $b(x,r) = Bxb_1(r)$  (i.e., a rate exhibiting linear particle volume dependence). The total droplet number and mass concentrations are denoted by  $N$  and  $M$ , respectively; i.e.,

$$N(r,z) = \int_0^{\infty} f(x,r,z) dx \quad (\text{A6})$$

$$M(r,z) = \int_0^{\infty} xf(x,r,z) dx \quad (\text{A7})$$

In the case of cross-sectionally uniform inlet concentration (i.e.,  $N = N_0$ ,  $M = M_0$ ), the following result can be obtained:

$$\begin{aligned} \frac{N}{N_0} = 1 + \frac{BM_0 z}{uN_0 R^2} 2 \int_0^R r' b_1(r') dr' + \\ \frac{BM_0}{DR^2 N_0} \sum_{i=2}^{\infty} \frac{2J_0(\lambda_i r)}{J_0^2(\lambda_i R)} \frac{1 - \exp\left[-\left(\frac{D}{u}\right) \lambda_i^2 z\right]}{\lambda_i^2} \\ \int_0^R r' b_1(r') J_0(\lambda_i r') dr' \quad (\text{A8}) \end{aligned}$$

The solutions derived here are the only possible exact solutions to the mathematical problem of breakage in turbulent pipe flow; actually, these are solutions to an oversimplified formulation of this problem.

## Literature Cited

- (1) Kostoglou, M.; Karabelas, A. J. On the attainment of steady state in turbulent pipe flow of dilute dispersions. *Chem. Eng. Sci.* **1998**, *53*, 505.
- (2) Hu, B.; Matar, O. K.; Hewitt, G. F.; Angeli, P. Population balance modelling of phase inversion in liquid-liquid pipeline flows. *Chem. Eng. Sci.* **2006**, *61*, 4994.
- (3) Nere, N. K.; Ramkrishna, D. Evolution of drop size distributions in fully developed turbulent pipe flow of a liquid-liquid dispersion by breakage. *Ind. Eng. Chem. Res.* **2005**, *44*, 1187.
- (4) Ramkrishna, D.; Nere, N. K. On evolution of drop size distributions in turbulent pipe flow revisited. *Ind. Eng. Chem. Res.* **2006**, *45*, 7673.



- (5) Nere, N. K.; Ramkrishna, D. Solution of population balance equation with pure aggregation in a fully developed turbulent pipe flow. *Chem. Eng. Sci.* **2006**, *71*, 96.
- (6) Karabelas, A. J. Vertical distribution of dilute suspensions in turbulent pipe flow. *AIChE J.* **1977**, *23*, 426.
- (7) Kostoglou, M.; Karabelas, A. J. Analytical treatment of fragmentation—diffusion population balance. *AIChE J.* **2004**, *50*, 1746.
- (8) Wilcox, D. C. *Turbulence Modeling for CFD*, Second Edition; DCW Industries, Inc.: La C  nada, CA, 1998.
- (9) Hrenya, C. M.; Bolio, E. J.; Chakrabarti, D.; Sinclair, J. L. Comparison of low Reynolds number  $k$ - $\epsilon$  turbulent models in predicting fully developed pipe flow. *Chem. Eng. Sci.* **1995**, *50*, 1923.
- (10) Myong, H. K.; Kasagi, N. A new approach to the improvement of  $k$ - $\epsilon$  turbulence model for wall bounded shear flows. *J. Soc. Mech. Eng.* **1990**, *33*, 63.
- (11) Lai, Y. G.; So, R. M. On near wall turbulent flow modeling. *J. Fluid Mech.* **1990**, *221*, 641.
- (12) Laufer, J. The structure of turbulence in fully developed pipe flow. *Natl. Advis. Comm. Aeronaut., Rep.* **1954**, 1174.
- (13) Schildknecht, M.; Miller, J. A.; Meier, G. E. A. The influence of suction on the structure of turbulence in fully developed pipe flow. *J. Fluid Mech.* **1979**, *90*, 67.
- (14) Deen, W. M. *Analysis of Transport Phenomena*; Oxford University Press: New York, 1998.
- (15) Luo, H.; Svendsen, H. F. Theoretical model for drop and bubble breakup in turbulent dispersions. *AIChE J.* **1996**, *42*, 1225–1233.
- (16) Wang, T.; Wang, J.; Jin, J. A novel theoretical breakup kernel function for bubbles/droplets in a turbulent flow. *Chem. Eng. Sci.* **2003**, *58*, 4629.
- (17) Wang, T.; Wang, J.; Jin, J. An efficient numerical algorithm for “A novel theoretical breakup kernel function of bubble/droplet in a turbulent flow”. *Chem. Eng. Sci.* **2004**, *59*, 2593.
- (18) Kostoglou, M.; Karabelas, A. J. Towards a unified framework for the derivation of breakage functions based on the statistical theory of turbulence. *Chem. Eng. Sci.* **2005**, *60*, 6584.
- (19) Lehr, F.; Mewes, D.; Millies, M. Bubble-Size distributions and flow fields in bubble columns. *AIChE J.* **2002**, *48*, 2426.
- (20) Vankova, N.; Tcholakova, S.; Denkov, N. D.; Ivanov, I. B.; Vulchev, V. D.; Danner, T. Emulsification in turbulent flow. 1. Mean and maximum drop diameters in inertial and viscous regimes. *J. Colloid Interface Sci.* **2007**, *312*, 363.
- (21) Vankova, N.; Tcholakova, S.; Denkov, N. D.; Vulchev, V. D.; Danner, T. Emulsification in turbulent flow. 2. Breakage rate constants. *J. Colloid Interface Sci.* **2007**, *313* (2), 612.
- (22) Tcholakova, S.; Vankova, N.; Denkov, N. D.; Ivanov, I. B.; Danner, T. Emulsification in turbulent flow. 3. Daughter drop size distribution. *J. Colloid Interface Sci.* **2007**, *310*, 570.
- (23) Chatzi, E. G.; Gavrielides, A. D.; Kiparissides, C. Generalized model for prediction of the steady state drop size distributions in batch stirred vessels. *Ind. Eng. Chem. Res.* **1989**, *28*, 1704.
- (24) Sathyagal, A. N.; Ramkrishna, D.; Narsimhan, G. Droplet breakage in stirred dispersions. Breakage functions from experimental drop-size distributions. *Chem. Eng. Sci.* **1996**, *51*, 1377.
- (25) Raikar, N. B.; Bhatia, S. R.; Malone, M. F.; Henson, M. A. Self-similar inverse population balance modeling for turbulently prepared batch emulsions: Sensitivity to measurement errors. *Chem. Eng. Sci.* **2006**, *61*, 7421.
- (26) Kostoglou, M. On the evolution of particle size distribution in pipe flow of dispersions undergoing breakage. *Ind. Eng. Chem. Res.* **2006**, *45*, 2143.

Received for review March 9, 2007  
 Revised manuscript received July 23, 2007  
 Accepted August 28, 2007

IE070360W